Available online at www.sciencedirect.com
SCIENCE DIRECT®
Journal of Power Sources 134 (2004) 103–109
JOURNAL OF POWER SOURCES
www.elsevier.com/locate/jpowsour

Characteristics of $LiCoO_2$ thin film cathodes according to the annealing ambient for the post-annealing process

Woo-Seong Kim*

GISANBTC Co. Ltd., Technical Center, Kwangju 500-110, South Korea

Received 16 December 2003; accepted 13 February 2004

Available online 7 Jun 2004

Abstract

As-grown, amorphous $LiCoO_2$ cathodes grown using a sputtering system were annealed in the temperature range of 650–900 °C under an Ar and O_2 ambients, respectively, in order to obtain crystalline $LiCoO_2$ cathodes. The resulting cathodes were then systematically compared with respect to their charge–discharge properties. The post-annealing process under an O_2 ambient resulted in superior cycling performance and thermal stability at high temperature than the Ar ambient. This effect is discussed in terms of grain boundary, surface roughness, and the outdiffusion of oxygen.

Keywords: Thin film; Battery; Cathode; Sputter; Charge–discharge; Capacity

1. Introduction

A rechargeable thin film battery has great potential, in terms of applications to electronic devices such as micro-electro-mechanical system (MEMS), smart cards, and micro power sources for metal-oxide-semiconductor (MOS) capacitor [1–3]. A major reason for this is that it is completely solid state, and no gas is generated during operation, and can be fabricated in a variety of shapes.

Crystalline $LiCoO_2$ is widely used as the cathode material in secondary rechargeable lithium batteries [4–6]. This material has a rhombohedral structure, with a hexagonal lattice, consisting of layers of close-packed oxygen ions separated by alternating layers of Li and Co ions. Nearly completely crystalline cathode films, for use in the thin film batteries, have been grown using sputtering system followed by post-annealing process [7–10]. As-grown $LiCoO_2$ films grown by the sputtering system are amorphous. Therefore, a post-annealing process is required in order to obtain the desired crystalline $LiCoO_2$ film. Post-annealing is typically conducted at about 700–800 °C under air, O_2, or N_2 [7,8]. We have previously examined the effect of the annealing process for other materials [11] and concluded that the annealing ambient can lead to significant changes in the physical and electrical properties of materials. However, the effects of annealing ambient on $LiCoO_2$ cathodes during the post-annealing process for rechargeable thin film batteries have not yet been systematically investigated.

In this paper, we report on a systematic investigation of the effects of the annealing ambient during the post-annealing of $LiCoO_2$ cathode films grown by the sputtering system. The effects of annealing ambient during the post-annealing process were compared with each other from the standpoint of charge–discharge properties and thermal stability.

2. Experimental

$LiCoO_2$ films were grown using an rf magnetron sputtering system on Pt (3000 Å)/MgO (1000 Å)/Ti (300 Å) current collectors on Si(0 0 1) substrate, where the MgO and Ti served as the diffusion barrier and adhesive layer, respectively. The target was a 2 in. $LiCoO_2$ and the base pressure was below 5×10^{-3} mTorr to eliminate impurities in the vacuum chamber. The distance between the sputter gun and the substrate was 5 cm. Prior to $LiCoO_2$ growth, a pre-sputtering treatment was performed for 30 min at 80 W under Ar pressure in order to eliminate impurities on the $LiCoO_2$ target. $LiCoO_2$ films were then deposited for 60 min at 80 W under a working pressure of 5 mTorr. The growth temperature was about 10 °C and the flow of Ar and O_2 was 30 and 10 SCCM, respectively. The deposition rate was about 16.7 Å/min. The initial, as-grown $LiCoO_2$ films were amorphous. To obtain

* Fax: +82-62-269-8016.
E-mail address: kws0720@hanmail.net (W.-S. Kim).

0378-7753/$ – see front matter © 2004 Elsevier B.V. All rights reserved.
doi:10.1016/j.jpowsour.2004.02.035

the desired degree of crystallinity in the $LiCoO_2$ films, the films were annealed for 30 min at 650, 750, 800, 850, and 900 °C under an Ar or O_2 ambients of 10 mTorr, respectively. Before annealing the samples, the pressure of the annealing chamber was reduced to below 2×10^{-3} mTorr in order to accurately compare the effects of the annealing ambient. The temperature overshoots were very small (<5 °C) and steady-state temperatures were achieved in 1 min. After each post-annealing process, the $LiCoO_2$ films were characterized using a surface profiler (α-step) for thickness, by atomic force microscopy (AFM, Park Sci. & Instrument) to evaluate surface roughness and surface morphology, and by X-ray diffraction (XRD) for internal structure. All the $LiCoO_2$ films used had a thickness of 0.1 μm.

The electrochemical reversibility of Li intercalation in $LiCoO_2$ films was measured by two-electrode cells and charge–discharge cycler (WBCS 3000, Won-A Tech., Korea). A Li foil and $LiCoO_2$ film were used as anode and cathode, respectively. The electrolyte was 1 M $LiCF_3SO_3$ dissolved in propylene carbonate (PC) + 1,2-dimethoxyethane (DME) (1:2) and all the cells were prepared in a dry room. All the cells were cycled at room temperature. The cells were initially charged to 4.2 V at 5 μA/cm^2 and held at 4.2 V until the current decreased below 1 μA/cm^2. The cells were then discharged from 4.2 to 3 V at 5 μA/cm^2. Finally, the cells were charged and discharged at current rate of 10 μA/cm^2 and cycled to 40 times.

3. Results and discussion

Fig. 1 shows XRD data for the $LiCoO_2$ films which were annealed for 30 min under Ar (a) and O_2 (b) ambients, respectively. The asterisk (*) peak positions are high-energy peaks for the Si substrate, which are visible by high-flux X-ray equipment with a graphite monochromator. The $LiCoO_2$ films were annealed at 750 °C for both ambient had amorphous structure. Crystallization of the $LiCoO_2$ films was observed at the temperatures above 800 °C, as well as for the components of the current collector and the reaction peaks between them.

Fig. 2 shows the discharge curves as a function of current rate for the $LiCoO_2$ films annealed at 750 and 850 °C, respectively, under Ar (a, b) and O_2 (c, d) ambients. Fig. 2(a) and (c) shows smooth discharge curves with no plateau, indicating that the $LiCoO_2$ films annealed at 750 °C have an amorphous structure. In contrast, Fig. 2(b) and (d) shows discharge curves which are typical of crystalline $LiCoO_2$ films and have plateaus at 3.93, 4.07, and 4.17 V indicating a phase transformation [6,7]. Fig. 2 also shows that crystalline $LiCoO_2$ films have a better rate performance than amorphous $LiCoO_2$ films. The lithium diffusivity in crystalline $LiCoO_2$ film is higher than that of amorphous $LiCoO_2$ film [7], indicating that a crystalline $LiCoO_2$ film has a lower cell resistance and, as a result, a better rate performance (see discharge curves for the current rates of 5 and 10 μA/cm^2).

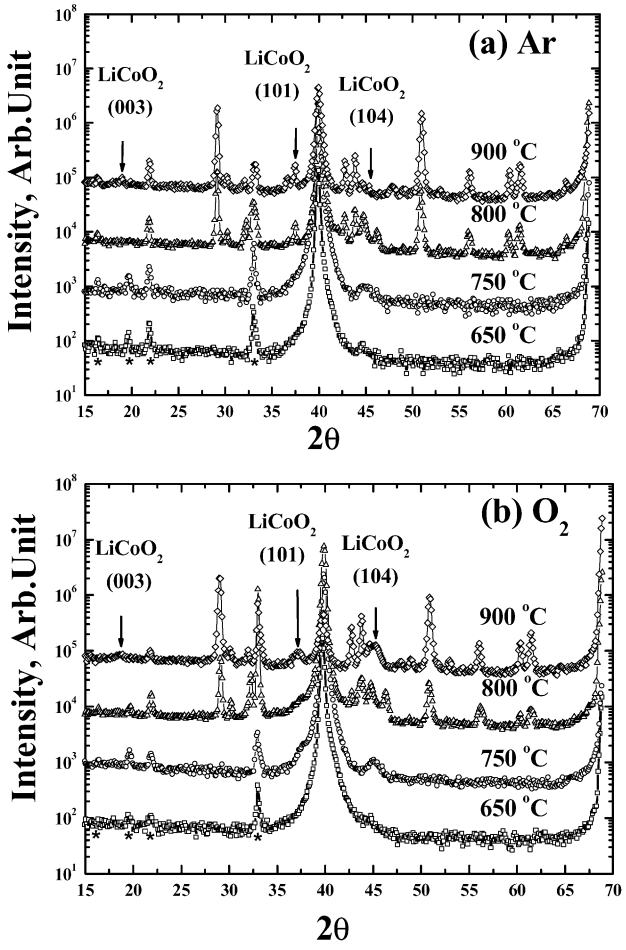

Fig. 1. XRD data for $LiCoO_2$ films annealed under (a) Ar and (b) O_2 ambients, respectively.

The $LiCoO_2$ films which were annealed at 800 °C showed a medium shape between the discharge curves of crystalline and amorphous $LiCoO_2$ films (not shown here), indicating an uncompleted crystallization of the $LiCoO_2$ film. These films showed poorer rate performance than the crystalline $LiCoO_2$ films annealed at 850 °C. The differences between the $LiCoO_2$ films annealed using Ar and O_2 ambients will be discussed below.

Fig. 3 shows AFM data and images of $LiCoO_2$ films. Fig. 3(a) shows the root-mean-square (rms) roughness with increasing annealing temperatures under Ar and O_2 ambients. Fig. 3(b)–(d) shows AFM images of the $LiCoO_2$ films annealed at 750 and 800 °C under Ar (b, d) and O_2 (c, e), respectively. The surface roughness remained unchanged for temperatures up to 750 °C. When the annealing temperature was increased above 800 °C, however, significant surface roughening was observed. The rms roughness had similar values for temperatures above 800 °C. Surface roughening leads to an increase in specific surface area. In addition, because the diffusivities (D) between surface, grain boundary, and lattice generally have the relationship of $D_s > D_{gb} > D_{latt}$ [12], surface roughening may increase the flux of Li

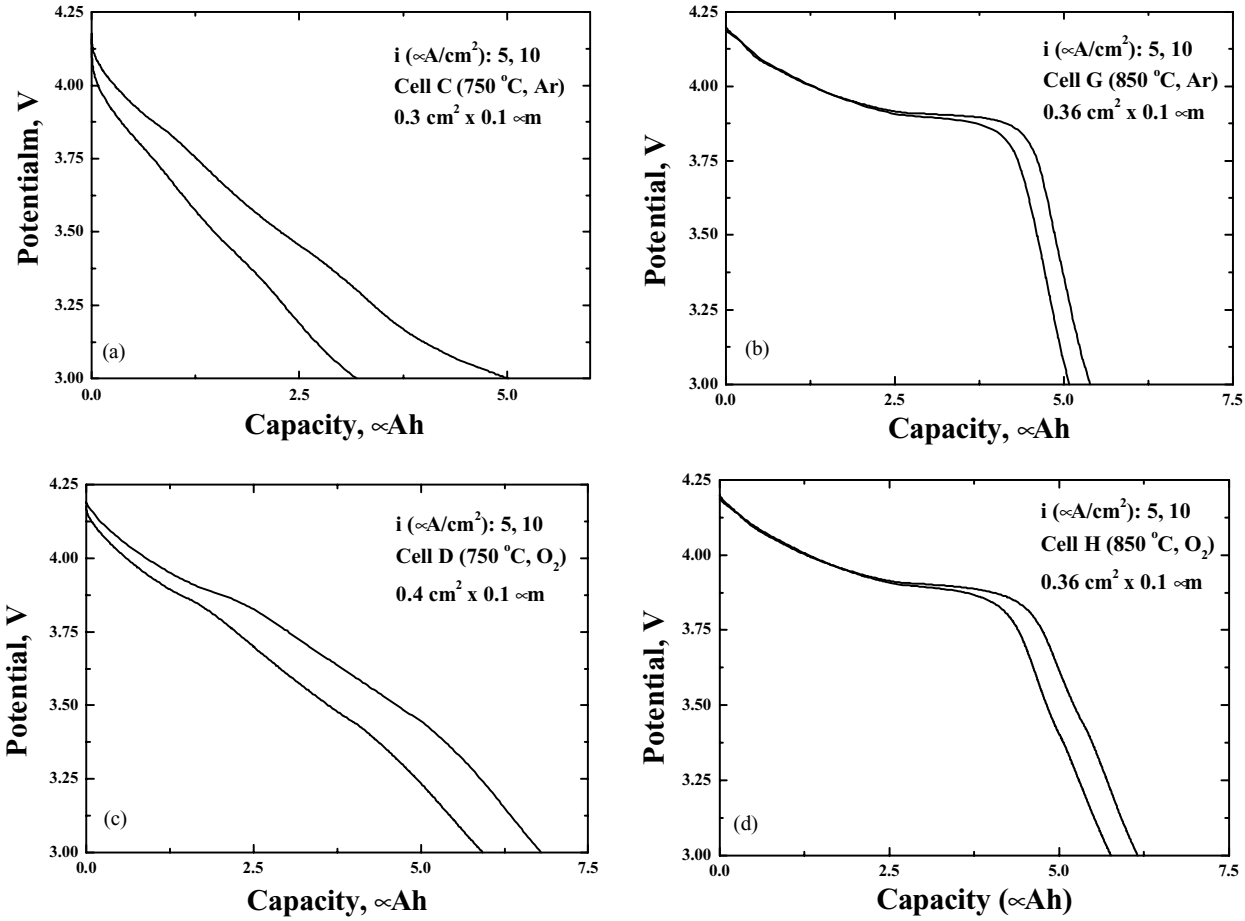

Fig. 2. Discharge curves as a function of current rates for $LiCoO_2$ films annealed at 750 and 850 °C, respectively, under Ar (a, b) and O_2 (c, d) ambients.

ions at the interface. Fig. 3(b)–(d) clearly shows the surface reconstruction or agglomeration of $LiCoO_2$ at 800 °C, indicating that the $LiCoO_2$ films now existed in the crystalline state.

Fig. 4 shows the initial coulombic efficiency (CE) (a) at an initial current rate of 5 μA/cm^2, specific discharge capacities (b, c) at an initial current rate of 5 μA/cm^2 and at an initial current rate of 10 μA/cm^2 after 5 μA/cm^2 cycling, respectively. In the case of the Ar ambient in Fig. 4(a), the initial CE was increased to 800 °C. We conclude that this is due to the increased active volume for Li insertion, as the result of increased surface roughening and the phase transformation from amorphous structure to crystalline structure. As the annealing temperature was increased from 800 to 900 °C, the initial CE was slightly decreased at 850 °C and significantly decreased at 900 °C, as shown in Fig. 4(a). This suggests that oxygen diffuses out of the $LiCoO_2$ films during the annealing at high temperature, which may cause cathode degradation. In contrast, the initial CE was gradually increased to 900 °C in the case of O_2 ambient. This indicates that the outdiffusion of oxygen from the $LiCoO_2$ film during the post-annealing process might be restricted due to the decreased oxygen vapor pressure of the $LiCoO_2$ films under the O_2 ambient. The CE values for the $LiCoO_2$ films annealed at 800 and 850 °C under an O_2 ambient were lower than that of $LiCoO_2$ films annealed under an Ar ambient. This indicates that lithium oxides such as Li_2O may be formed on the surface of the high temperature annealed $LiCoO_2$ film under an O_2 ambient and that a simultaneous decomposition of the Li oxides occurred during the initial charging, because the Li oxides are decomposed above about 1 V [13,14]. The issue of how the oxygen, formed by the decomposition of Li oxides during initial charging, participates in the long-term cycling performance of the cell is studied underway. Fig. 4(b) and (c) shows that specific discharge capacities have quite high values, compared with the theoretical value (70.69 μAh/cm^2 μm calculated for 0.5Li [15]). Dudney reported that this could be the result of reactions involving lithium and the liquid electrolyte [10]. Fig. 4(b) and (c) shows that specific discharge capacities were increased to 800 °C for $LiCoO_2$ films annealed under an Ar ambient due to easier insertion of lithium, as the result of increased surface roughening and the phase transformation, as mentioned above. However, at the temperatures above 800 °C, the specific discharge capacity was slightly decreased at 850 °C and substantially decreased at 900 °C for $LiCoO_2$ films annealed under an Ar ambient, due to degradation of the cathode, caused by the significant out-

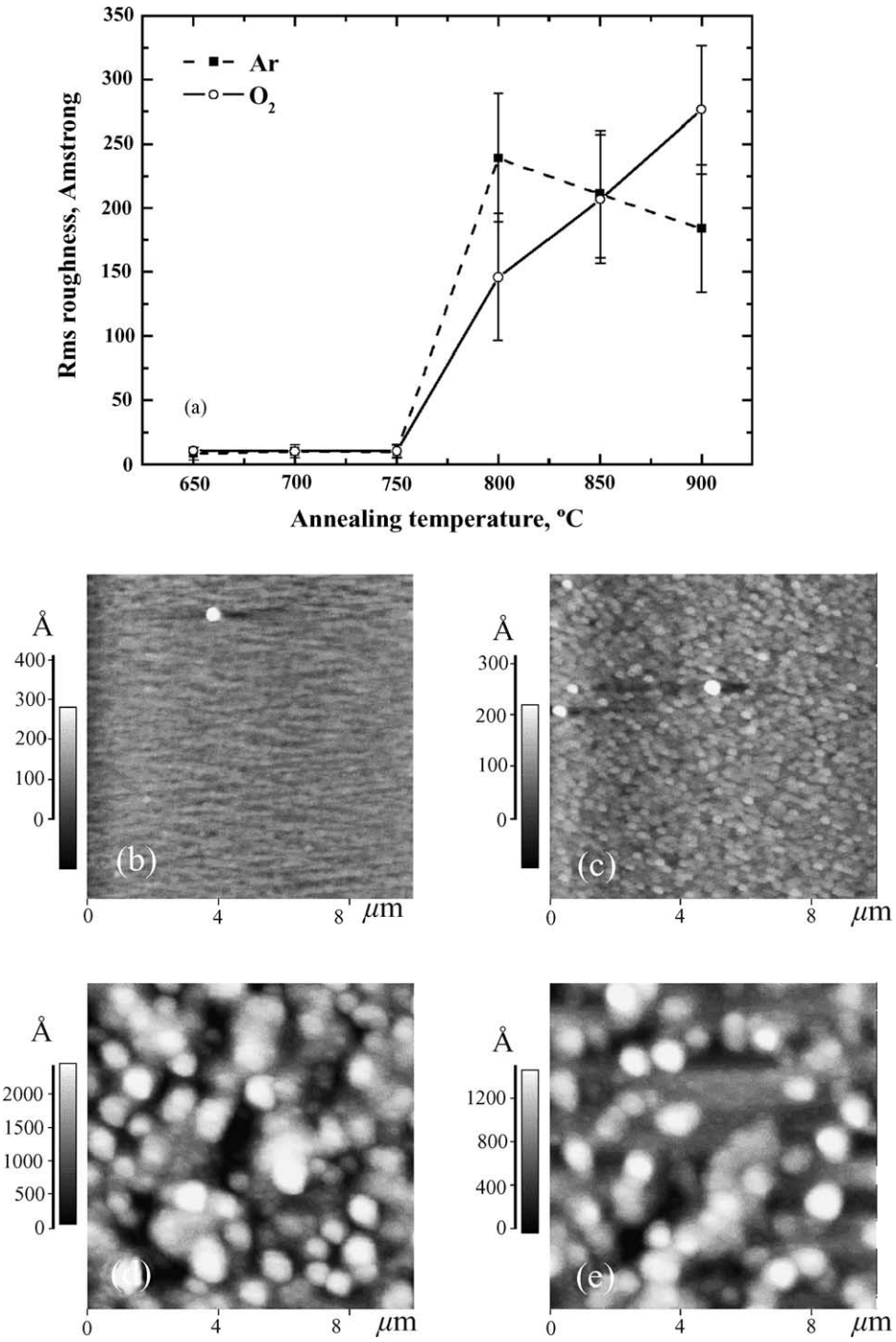

Fig. 3. AFM data for the annealed $LiCoO_2$ films: (a) rms surface roughness as a function of annealing temperature; (b)–(e) AFM images for the samples annealed at 750 and 800 °C, respectively, under Ar (b, d) and O_2 (c, e) ambients.

diffusion of oxygen from $LiCoO_2$ films. Fig. 4(b) and (c) also shows that specific discharge capacities were increased to 800 or 850 °C for $LiCoO_2$ films annealed under an O_2 ambient but were only slightly decreased at 900 °C. Generally, the higher the annealing temperature, the larger the grain size, indicating the decrease of the grain boundary density. A slight decrease in specific discharge capacity at 900 °C may have occurred because of the similar rms surface roughness in the range of 800–900 °C and the density decrease of the grain boundary, which facilitates the pathway of Li into $LiCoO_2$ films. Compared with the result relative to $LiCoO_2$ films annealed at 900 °C under an Ar ambient, this clearly indicates that the post-annealing process under an O_2 ambient restricts the diffusion of oxygen out of the films and the degradation of the $LiCoO_2$ films.

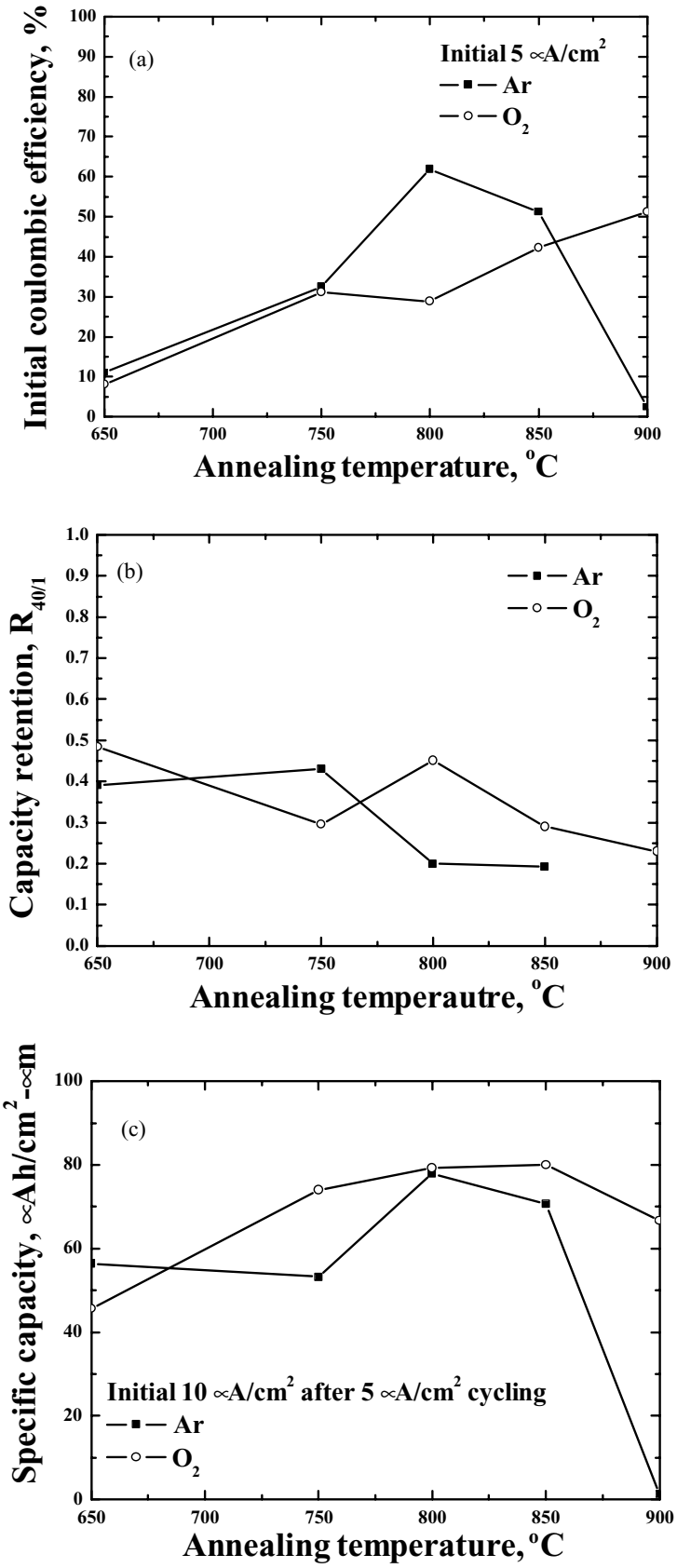

Fig. 4. Initial CE (a) at initial 5 μA/cm^2 and specific discharge capacities (b, c) at initial 5 μA/cm^2 and initial 10 μA/cm^2 after first 5 μA/cm^2 cycling, respectively.

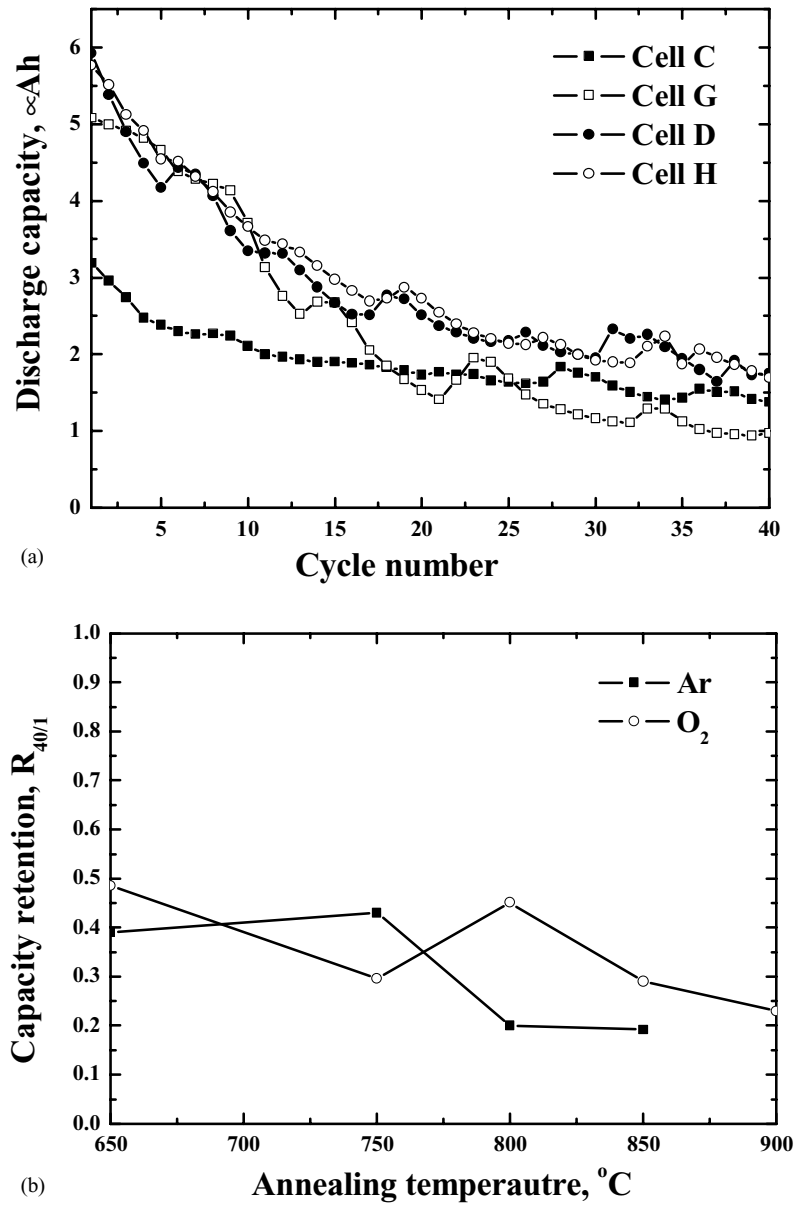

Fig. 5. Long-term cycling performance: (a) cycling performance for the samples shown in Fig. 2; (b) discharge capacity retention ($R_{40/1}$) for the $LiCoO_2$ films with the annealing temperature.

Fig. 5 shows data on long-term cycling performance. Fig. 5(a) and (b) shows cycling performance up to 40 times for the samples shown in Fig. 2 and the discharge capacity retention ($R_{40/1}$), ratio of 1–40 cycles, as a function of annealing temperature, respectively. The capacity fade phenomena during cycling are generally caused by interface degradation between $LiCoO_2$ film and the electrolyte, because the concentration variation of Li ions is the highest at the interface during the cycling [7]. Fig. 5(b) shows that $R_{40/1}$ is generally gradually decreased to 850 °C in both Ar and O_2 ambients, due to the increased grain size and surface roughening. The increased specific surface area, caused by surface roughening, may stimulate interface degradation to a great extent during cycling. This causes an increase in cell resistance with cycling, in spite of the increased initial specific discharge capacities as shown in Fig. 4(b) and (c). In the case of the $LiCoO_2$ film annealed at 900 °C under an O_2 ambient, $R_{40/1}$ had a slightly lower value than that annealed at 850 °C under an O_2 ambient. However, the $LiCoO_2$ film annealed at 900 °C under an Ar ambient was cycled up to 10 times and, then, not cycled, due to the degradation of $LiCoO_2$ film caused by the diffusion of oxygen out of the films, as mentioned above.

From the above discussion, the post-annealing process under O_2 ambient leads to better cycling performance and thermal stability at high temperatures, compared to the use of an inert Ar ambient.

4. Conclusions

The effects of annealing ambient during the post-annealing process for the $LiCoO_2$ films grown by sputtering system were systematically investigated. Post-annealing process under an O_2 ambient leads to superior long-term cycling performance and thermal stability above 800 °C, compared with the use of an inert Ar ambient. This may be due to cathode degradation caused by diffusion of oxygen out of the $LiCoO_2$ films annealed at high temperature under an inert Ar ambient. Surface roughening above 800 °C increased the initial specific capacity but led to worse long-term cycling performance.

Acknowledgements

This work was supported by the Ministry of Commerce, Industry and Energy in Korea.

References

[1] K. Kanehori, K. Matsumoto, K. Miyauci, T. Kudo, Solid State Ionics 9–10 (1983) 1445.
[2] J.B. Bates, Proceedings of the Symposium on Thin Film Solid Ionics Devices and Materials, vol. 95-22, The Electrochemical Society Inc., Pennington, 1996, pp. 148–152.
[3] J.B. Bates, G.R. Gruzalski, N.J. Dudney, C.F. Luck, X.-H. Yu, S.D. Jones, Solid State Tech. 36 (1993) 59.
[4] M. Winter, J.O. Besenhard, M.E. Spahr, P. Novak, Adv. Mater. 10 (1998) 725.
[5] K. Mizushima, P.C. Jones, P.J. Wiseman, J.B. Goodenough, Mater. Res. Bull. 15 (1980) 783.
[6] J.N. Reimers, J. Dahn, Mater. Res. Bull. 139 (1992) 2091.
[7] B. Wang, J.B. Bates, F.X. Hart, B.C. Sales, R.A. Zuhr, D. Robertson, J. Electrochem. Soc. 143 (1996) 3203.
[8] J.K. Lee, S.J. Lee, H.K. Baik, H.Y. Lee, S.W. Jang, S.M. Lee, Electrochem. Solid-State Lett. 2 (1999) 512.
[9] F.K. Shokoohi, J.M. Tarascon, B. Wilkens, J. Appl. Phys. Lett. 59 (1991) 1260.
[10] N.J. Dudney, J. Power Sources 89 (2000) 176.
[11] K.S. Ahn, D.J. Kim, Y.T. Moon, H.G. Kim, S.J. Park, J. Vac. Sci. Technol. B 19 (2001) 215.
[12] D.A. Porter, K.E. Easterling, Phase Transformations in Metals and Alloys, second ed., Chapman & Hall, London, 1992, pp. 98–103.
[13] I.A. Courtney, J.R. Dahn, J. Electrochem. Soc. 144 (1997) 2943.
[14] H. Morimoto, M. Nakai, M. Tatsumisago, T. Minami, J. Electrochem. Soc. 146 (1999) 3970.
[15] P.N. Kumta, D. Gallet, A. Waghray, G.E. Blomgren, M.P. Setter, J. Power Sources 72 (1998) 91.